FUNCTION™ american physiological society

FUNCTION, 2022, 3(4): zqac034

https://doi.org/10.1093/function/zqac034
Advance Access Publication Date: 4 July 2022
Original Research

RESEARCH ARTICLE

Deletion of Thioredoxin Reductase Disrupts Redox Homeostasis and Impairs β-Cell Function

Jennifer S. Stancill[1,*], Polly A. Hansen[1], Angela J. Mathison[2,3], Edward E. Schmidt[4,5], John A. Corbett[1,*]

[1]Department of Biochemistry, Medical College of Wisconsin, Milwaukee, Wisconsin, 53226, USA, [2]Genomic Sciences and Precision Medicine Center, Medical College of Wisconsin, Milwaukee, WI 53226, USA, [3]Division of Research, Department of Surgery, Medical College of Wisconsin, Milwaukee, WI 53226, USA, [4]Department of Microbiology and Cell Biology, Montana State University, Bozeman, MN 59717, USA and [5]Redox Biology Laboratory, University of Veterinary Medicine, Budapest 1078, Hungary

*Address correspondence to J.A.C. (e-mail: jcorbett@mcw.edu), J.S.S. (e-mail: jstancill@mcw.edu)

Abstract

Reactive oxygen species (ROS) have been implicated as mediators of pancreatic β-cell damage. While β-cells are thought to be vulnerable to oxidative damage, we have shown, using inhibitors and acute depletion, that thioredoxin reductase, thioredoxin, and peroxiredoxins are the primary mediators of antioxidant defense in β-cells. However, the role of this antioxidant cycle in maintaining redox homeostasis and β-cell survival *in vivo* remains unclear. Here, we generated mice with a β-cell specific knockout of thioredoxin reductase 1 (*Txnrd1*$^{fl/fl}$; *Ins1*$^{Cre/+}$, βKO). Despite blunted glucose-stimulated insulin secretion, knockout mice maintain normal whole-body glucose homeostasis. Unlike pancreatic islets with acute *Txnrd1* inhibition, βKO islets do not demonstrate increased sensitivity to ROS. RNA-sequencing analysis revealed that *Txnrd1*-deficient β-cells have increased expression of nuclear factor erythroid 2-related factor 2 (Nrf2)-regulated genes, and altered expression of genes involved in heme and glutathione metabolism, suggesting an adaptive response. *Txnrd1*-deficient β-cells also have decreased expression of factors controlling β-cell function and identity which may explain the mild functional impairment. Together, these results suggest that *Txnrd1*-knockout β-cells compensate for loss of this essential antioxidant pathway by increasing expression of Nrf2-regulated antioxidant genes, allowing for protection from excess ROS at the expense of normal β-cell function and identity.

Submitted: 29 April 2022; **Revised:** 17 June 2022; **Accepted:** 27 June 2022

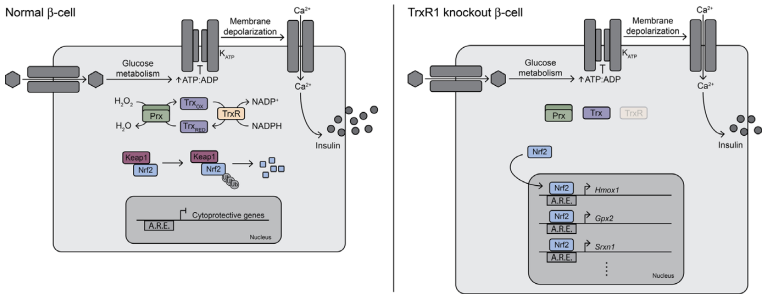

Key words: β-cells; radicals; thioredoxin reductase; diabetes; insulin secretion

Introduction

Accumulation of reactive oxygen species (ROS), like superoxide and hydrogen peroxide, causes oxidation of lipids, proteins, and DNA, and may contribute to β-cell damage,[1] and numerous studies have reported increased oxidative damage in islets from diabetic rodents and patients.[2–10] Superoxide is largely produced during mitochondrial oxidative phosphorylation.[11,12] In β-cells, glycolysis is coupled to oxidative phosphorylation such that most of the carbons in glucose are oxidized to CO_2 on supply of the sugar substrate.[13–15] This metabolic flux allows for β-cells to respond to blood glucose changes with changes in insulin secretion that are controlled by glucose sensing and the rates of oxidation.[16] In diabetes, when blood glucose is chronically elevated, electron leak during increased oxidative phosphorylation may increase ROS, contributing to β-cell damage.[17,18]

β-cells are considered vulnerable to oxidative stress due to lower expression levels of antioxidant enzymes compared to levels found in liver and kidney.[19–22] Indeed, overexpression of superoxide dismutase, catalase, glutathione peroxidase (Gpx), or thioredoxin (Trx) in mouse β-cells protects against various forms of oxidative damage.[23–27] Together, these studies suggest that β-cells are sensitive to ROS because of the relatively weak antioxidant defense, and damage induced by oxidants has been implicated in the loss of functional mass during disease development. However, from an evolutionary perspective, there are several logical reasons why β-cells should be protected from ROS in that: they produce insulin, a hormone that is essential for survival; they have limited replicative capacity; and they rely on a ROS-producing pathway (mitochondrial oxidation) to secrete insulin. Consistent with the view that β-cells are protected from oxidative damage, they express peroxiredoxins (Prx), Trx, and thioredoxin reductase (TrxR), which together form an antioxidant cycle that reduces hydrogen peroxide, peroxynitrite, and lipid peroxides utilizing NADPH.[28–30] In this cycle, Prx reduces an oxidant but becomes oxidized and inhibited in the process. Via disulfide exchange, Trx reduces Prx, and TrxR, in turn, reduces Trx, allowing the cycle to continue.

Recent studies have shown that INS 832/13 insulinoma cells and rat islets can detoxify micromolar levels of hydrogen peroxide when delivered continuously, but not as a bolus.[28] When TrxR is either inhibited or depleted, insulinoma cells and rat islets become significantly sensitized to hydrogen peroxide, exhibiting DNA damage and death at lower hydrogen peroxide concentrations than control cells.[28] These findings suggest that TrxR is necessary for β-cell detoxification of this oxidant. Further supporting this model, inhibition or depletion of cytoplasmic Prx1 (*Prdx1*) sensitizes insulinoma cells and rat islets to continuously-delivered hydrogen peroxide.[31] Although peroxynitrite has been suggested as a mediator of cytokine damage in β-cells, we have shown that β-cells utilize this same antioxidant pathway to protect themselves from this potent oxidant.[31] Finally, increased levels of *Txnip*, an inhibitor of Trx, are associated with increased β-cell apoptosis while *Txnip* deficiency protects against development of diabetes in mice,[32–35] suggesting that the Trx/Prx antioxidant pathway is necessary for β-cell survival. These exciting studies suggest that β-cells maintain a robust antioxidant defense system requiring TrxR and Prx to protect themselves from damage.

Although inhibition or knockdown of TrxR or Prx1 sensitizes insulinoma or rat islet cells to oxidants,[28,31] we do not know if this effect can be recapitulated *in vivo* by specific genetic disruption. Here, we generated a mouse model with a β-cell-specific knockout of the cytoplasmic TrxR, *Txnrd1* (*Txnrd1*$^{fl/fl}$; *Ins1*$^{Cre/+}$, βKO) to determine how removal of this essential antioxidant pathway affects β-cell survival and function. βKO islets have blunted glucose-stimulated insulin secretion, but βKO mice maintain normal glucose homeostasis, insulin content, and islet architecture. In contrast to acute TrxR inhibition by auranofin (AFN), βKO islets are not sensitized to continuously-delivered hydrogen peroxide or peroxynitrite. Transcriptome analysis of FACS-purified *Txnrd1*-deficient β-cells revealed constitutive stabilization of transcription factor nuclear factor erythroid 2-related factor 2 (Nrf2) and enhanced expression of Nrf2-regulated genes, including those involved in heme and glutathione metabolism, suggesting an adaptive redox homeostasis shift. There is also decreased expression of critical identity factors *Mafa*, *Slc2a2*, *Ucn3*, and *Pdx1* in *Txnrd1*-deficient β-cells. These findings suggest that removal of the essential antioxidant TrxR necessitates a shift in redox homeostasis at the expense of normal β-cell function and identity.

Materials and Methods

Animals and Reagents

Txnrd1^{fl} mice (JAX Stock No. 028283)[36] were backcrossed with C57BL/6 mice for nine generations prior to breeding with *ROSA*^{mTmG} mice.[37] *ROSA*^{mTmG} mice (JAX Stock No. 007676) and *Ins1*$^{Cre/+}$mice[38] (JAX Stock No. 026801) were obtained from Jackson Laboratories. All mouse lines studied are maintained on a C57BL/6 congenic background and were backcrossed to this strain for at least ten generations prior to arriving to our colony. Experimental animals were 10–20 wks of age. All animal use and experimental procedures were approved by the Institutional Animal Care and Use Committees at the Medical College of Wisconsin. Rat insulinoma INS 832/13 cells were obtained from Chris Newgard (Duke University, Durham, NC, USA).[39] Connaught Medical Research Laboratories (CMRL) 1066 medium, Hank's Balanced Salt Solution (HBSS), Roswell Park

Memorial Institute (RPMI) 1640 medium L-glutamine, sodium pyruvate, HEPES, penicillin and streptomycin, Versene (0.48 mM EDTA), DNase, 4',6-diamidino-2-phenylindole (DAPI), ProLong Gold Antifade Mountant with DAPI, and SYTOX Green nucleic acid stain were purchased from ThermoFisher Scientific (Waltham, MA, USA). Fetal bovine serum (FBS) is from HyClone (Logan, UT, USA). Flow Cytometry Buffer was obtained from R&D Systems (Minneapolis, MN, USA). Dipropylenetriamine NONOate (DPTA/NO) and Aem1 were supplied by Cayman Chemical (Ann Arbor, MI, USA). AFN, glucose oxidase, menadione, hydrogen peroxide solution, and β-mercaptoethanol were purchased from Sigma-Aldrich (St. Louis, MO, USA). Aem1 was dissolved in DMF at a concentration of 10 mM before further dilution in cell culture medium. AFN was dissolved in DMSO at a concentration of 5 mM before further dilution. Glucose oxidase was solubilized in 0.05 M sodium acetate buffer at a concentration of 1 mg/mL before further dilution in cell culture medium. SYTOX Green was dissolved in DMSO at a concentration of 5 mM prior to use.

Islet Isolation, Culture, Dispersion, and Oxidant Treatment

Pancreatic islets were isolated from mice by collagenase digestion and were cultured at 37°C and 5% CO_2 in CMRL supplemented with 10% heat-inactivated FBS and containing 5.5 mM glucose as previously described.[40] Prior to FACS purification or to oxidant treatment, islets were dispersed into single cells by incubation in Versene (0.48 mM EDTA) followed by agitation in 1 mg/mL trypsin in Ca^{2+}/Mg^{2+}-free HBSS. For assessment of oxidant sensitivity, dispersed islets were pretreated with 5 μM AFN (or 0.1% DMSO as a vehicle control) for 30 min before addition of glucose oxidase (15 mU/mL) or the combination of DPTA/NO (200 μM) and menadione (20 μM). Cells were treated with DPTA/NO and menadione for 1 h and with glucose oxidase for 30 min.

Insulinoma Cell Culture and Oxidant Treatment

INS 832/13 cells were cultured as previously described,[41] and were maintained at 37°C under an atmosphere of 95% air and 5% CO_2. To determine sensitivity to oxidants, cells were pretreated for 3 h with 0.1 μM AFN (or 0.002% DMSO as a vehicle control), 10 μM Aem1 (or 0.1% DMF as a vehicle control), or both inhibitors together before 4 h treatment with glucose oxidase (0–10 mU/mL). Inhibitors were present during glucose oxidase treatment. Cell death was determined by assessment of fluorescence of the SYTOX Green nucleic acid stain as previously described.[42]

Assessment of Insulin Content

Pancreata were harvested from Tx*nrd1*$^{fl/fl}$; *Ins1*$^{Cre/+}$ (βKO) or Tx*nrd1*$^{fl/fl}$; *Ins1*$^{+/+}$ (*fl/fl*) control mice, rinsed in PBS, blotted dry, and weighed. Insulin was extracted from whole pancreata or groups of 15 islets using acid ethanol as described previously.[43] Insulin content was determined using the supernatant by insulin ELISA (Crystal Chem, Downers Grove, IL, USA).

Insulin Secretion Assay

Islets from βKO or *fl/fl* control mice were isolated and insulin secretion was assessed as previously described.[44] Briefly, 15 islets per condition were incubated at 37°C in Krebs–Ringer phosphate buffer. Islets were pretreated for 30 min with 5 μM AFN or 0.1% DMSO. Islets were stimulated with 3 mM glucose, 20 mM glucose, or 3 mM glucose plus 30 mM KCl for 90 min. AFN or DMSO was present during the stimulation period. Insulin levels were determined by insulin ELISA (Crystal Chem, Downers Grove, IL, USA). Secreted insulin was normalized to total islet insulin content.

Glucose Tolerance Test and Plasma Insulin Assessment

Glucose tolerance was determined at 15 wk of age after a 4-h fast. Mice were given 2 g dextrose/kg body weight by intraperitoneal injection. Blood glucose was determined before glucose challenge and 15, 30, 60, and 120 min after injection. To determine plasma insulin levels, blood samples were collected from tail vein before and 15 min after administration of a 2 g/kg intraperitoneal injection of dextrose. Blood samples were kept on ice and centrifuged (15 min at 500 x g), and plasma was stored at −80°C. Plasma insulin was determined by ELISA (Crystal Chem, Downers Grove, IL, USA).

FACS Purification

Following overnight culture, islets were dispersed, filtered, and resuspended in Flow Cytometry Buffer containing 2 U/mL DNase (ThermoFisher Scientific, Waltham, MA, USA). Live GFP$^+$ and live Tomato$^+$ cell populations were collected directly into Buffer RLT (Qiagen, Germantown, MD, USA) supplemented with β-mercaptoethanol (final concentration 143 mM) using a FACSAria II (BD Biosciences, Franklin Lakes, NJ, USA) instrument. DAPI was used at a final concentration of 5 μg/mL to prevent collection of dead cells.

RNA Isolation and RNA-sequencing

Total RNA was isolated from FACS-purified cell populations using an RNeasy kit (Qiagen, Germantown, MD, USA). Genomic DNA was removed using the TURBO DNA-free Kit (ThermoFisher Scientific, Waltham, MA, USA). Library preparation and sequencing were completed by the Genomic Sciences and Precision Medicine Center (GSPMC) at the Medical College of Wisconsin. Briefly, cDNA was synthesized from 5–10 ng of input RNA using the SMARTseq Ultra Low Input workflow (Takara Bio Inc., San Jose, CA, USA) with libraries prepared and amplified with Nextera DNA Library kit (Illumina, San Diego, CA, USA). Paired-end sequencing was performed on the Illumina NovaSeq6000 with 100 bp reads generating ~30 million mapped reads per sample. MAP-RSeq.v3.0[45] was used to align reads to the reference genome (GRCm38.p6) and to return raw and normalized expression values. A pairwise method in EdgeR[46] for was used for differential expression analysis of protein-coding genes that had at least 1 read per million in at least 6 samples.

qRT-PCR

Thermo Scientific Maxima H Minus reverse transcriptase and oligo(dT)s were used to perform first-strand cDNA synthesis from total RNA purified from mouse islets or INS 832/13 cells. SsoFast EvaGreen supermix (Bio-Rad, Hercules, CA, USA) and a Bio-Rad CFX96 Real-Time system were used to perform quantitative PCR with primers purchased from Integrated DNA Technologies (Coralville, IA, USA). Sequences are listed in Supplementary Table S1. Gene expression was normalized to *Actb* using the comparative ΔCt method for relative quantification.[47]

Western Blot

Equal amounts of protein from islet or INS 832/13 cell lysates were resolved by SDS/PAGE under reducing conditions and transferred to nitrocellulose membranes. Proteins were detected using primary antibodies: mouse anti-Gapdh (anti-glyceraldehyde 3-phosphate dehydrogenase; 1:20,000; ThermoFisher Scientific, Waltham, MA, USA), mouse anti-α-tubulin (1:2,000; GeneTex, Irvine, CA, USA), rabbit anti-Txnrd1 (1:5,000; Proteintech, Rosemont, IL, USA), mouse anti-phospho-H2AX (Ser139, γH2AX ; 1:10,000; EMD Millipore, Billerica, MA, USA), rabbit anti-Nrf2 (200 ng/mL, previously described,[48]), and rabbit anti-HO-1 (1:1,000; StressGen, San Diego, CA, USA) Detection was performed by enhanced chemiluminescence[49] using species-specific HRP-conjugated donkey anti-mouse or donkey anti-rabbit (1:20,000) secondary antibodies (Jackson ImmunoResearch Laboratories, West Grove, PA, USA). Densitometry was determined using ImageJ software (National Institutes of Health, Bethesda, MD, USA).

Immunofluorescence Imaging

Mouse pancreata were fixed in 4% paraformaldehyde for 4 h, incubated in 30% sucrose, frozen in OCT solution, and sectioned at a depth of 4 μM. Sections were permeabilized with 0.1% Triton X-100 in PBS for 30 min and blocked using 1% BSA in PBS-T (0.2% Tween-20) for 1 h at room temperature. Primary antibodies were diluted in 1% BSA in PBS-T and were incubated overnight at 4°C. Secondary antibodies were diluted in 1% BSA in PBS-T and were incubated for 1 h at room temperature. Antibodies and dilutions were as follows: guinea pig anti-insulin (1:1,000; Dako Cytomation, Carpinteria, CA, USA), rabbit anti-glucagon (1:1,000; Linco, St. Charles, MO, USA), donkey anti-guinea pig conjugated to Alexa Fluor 488 (1:1,000; ThermoFisher Scientific, Waltham, MA, USA), and donkey anti-rabbit conjugated to Alexa Fluor 647 (1:1,000; ThermoFisher Scientific, Waltham, MA, USA). ProLong Gold Antifade Mountant with DAPI (ThermoFisher Scientific, Waltham, MA, USA) was added to slides prior to addition of coverslip and imaging. Grayscale images were captured using a Nikon A1 laser scanning confocal microscope and were pseudocolored using ImageJ software (National Institutes of Health).

Measurement of Total Glutathione

Total glutathione levels were measured in βKO or *fl/fl* control islets using a Glutathione Assay Kit (Cayman Chemical, Ann Arbor, MI, USA). Islets were deproteinated using 3% metaphosphoric acid followed by sonication and centrifugation. Total glutathione was assessed using the 5,5'-dithio-*bis*-2-(nitrobenzoic acid) (DTNB) and glutathione reductase enzymatic recycling method[50] and was normalized to total protein levels using a Pierce BCA Protein Assay Kit (ThermoFisher Scientific, Waltham, MA, USA). Three technical replicates of 50 islets each were averaged for every experimental replicate.

Statistical Analysis

Differentially expressed genes from RNA-sequencing data were determined with EdgeR using a negative binomial model and TMM (trimmed mean of M-values) normalization. An adjusted *P*-value <0.05 and at least a 2-fold change in expression was the threshold used to declare significance. For all other comparisons, GraphPad Prism software was used to make statistical comparisons between groups using an unpaired, two-tailed *t*-test or one- or two-way ANOVA with Šidák's multiple comparisons correction. *P*-value <0.05 was the threshold used to declare significance. Area under the curve of individual glucose tolerance tests was calculated using GraphPad Prism software.

Results

Generation of Mice With a β-cell-specific Knockout of *Txnrd1*

We recently showed, using rat and human insulinoma cells and rat islets, that β-cells utilize thioredoxin reductase 1 (*Txnrd1*) to protect against damage from continuously-delivered hydrogen peroxide.[28] However, the role of this enzyme in maintaining redox homeostasis and β-cell survival *in vivo* remains unclear. Total body knockouts of *Txnrd1* are lethal at embryonic day 9.5 in the mouse,[36] but a conditional knockout allele (*Txnrd1*^{fl}) has been used to generate viable tissue-specific knockouts.[36,51] To generate a β-cell-specific knockout model, *Txnrd1*$^{fl/fl}$ mice were bred to mice expressing *Cre* in the endogenous *Ins1* locus (*Ins1*$^{Cre/+}$)[38] to obtain *Txnrd1*$^{fl/fl}$; *Ins1*$^{Cre/+}$ (βKO) animals (Figure 1A). To facilitate identification of β-cells in which *Txnrd1* has been recombined, we utilized the *ROSA26*^{mTmG} allele,[37], a dual-color fluorescent *Cre* reporter. Cells that lack *Cre* recombinase express a membrane-bound Tomato fluorescent protein, and cells that express *Cre* express a cytoplasmic GFP (Figure 1A). Indeed, insulin-containing cells in control *fl/fl* animals (*Txnrd1*$^{fl/fl}$; *Ins1*$^{+/+}$) express Tomato, and GFP expression in βKO pancreatic sections is consistent with β-cell-specific expression (Figure 1B). Recombination of the *Txnrd1*^{fl} allele results in a non-functional mRNA product rather than complete elimination of *Txnrd1* mRNA.[36] Consistently, βKO islets have reduced thioredoxin reductase 1 (TrxR1) protein levels compared to *fl/fl* controls (Figure 1C and D). The low level of *Txnrd1* protein present in βKO islets can be attributed to expression in non-β-cells, likely α- or δ-cells, which maintain TrxR1 expression.

Thioredoxin provides electrons (obtained from NADPH via *Txnrd1*) to ribonucleotide reductase, the enzyme that catalyzes the generation of deoxyribonucleotides from ribonucleotides and is necessary for DNA replication.[52]. Indeed, whole-body depletion of either *Txn1* or *Txnrd1* causes early embryonic lethality in the mouse.[36,53] However, there is no difference in pancreatic or islet insulin content in βKO islets compared to *fl/fl* controls (Figure 1E and F), suggesting that *Txnrd1* depletion does not result in decreased β-cell expansion or increased β-cell death. Further, βKO islets display normal islet architecture, with a core of GFP-expressing cells (β-cells) surrounded by a mantle of glucagon-expressing α-cells (Figure 1G).

Effects of *Txnrd1* Inhibition or Depletion on β-cell Function and Glucose Homeostasis

Acute inhibition of TrxR by the small molecule inhibitor AFN or chronic depletion by genetic knockout (βKO) significantly blunts glucose-stimulated or membrane depolarization (KCl)-stimulated insulin secretion (Figure 2A), suggesting that TrxR activity is necessary for normal β-cell function. However, there is no difference in glucose tolerance following a 4-h fast nor in plasma insulin levels 15 min after glucose challenge in βKO mice compared to *fl/fl* controls (Figure 2B–E). Male βKO mice have a slight but significant increase in blood glucose levels compared to *fl/fl* controls following a 4-h fast, while female βKO mice do not (Figure 2F). However, no difference in random fed blood glucose levels between βKO mice and *fl/fl* controls was observed in

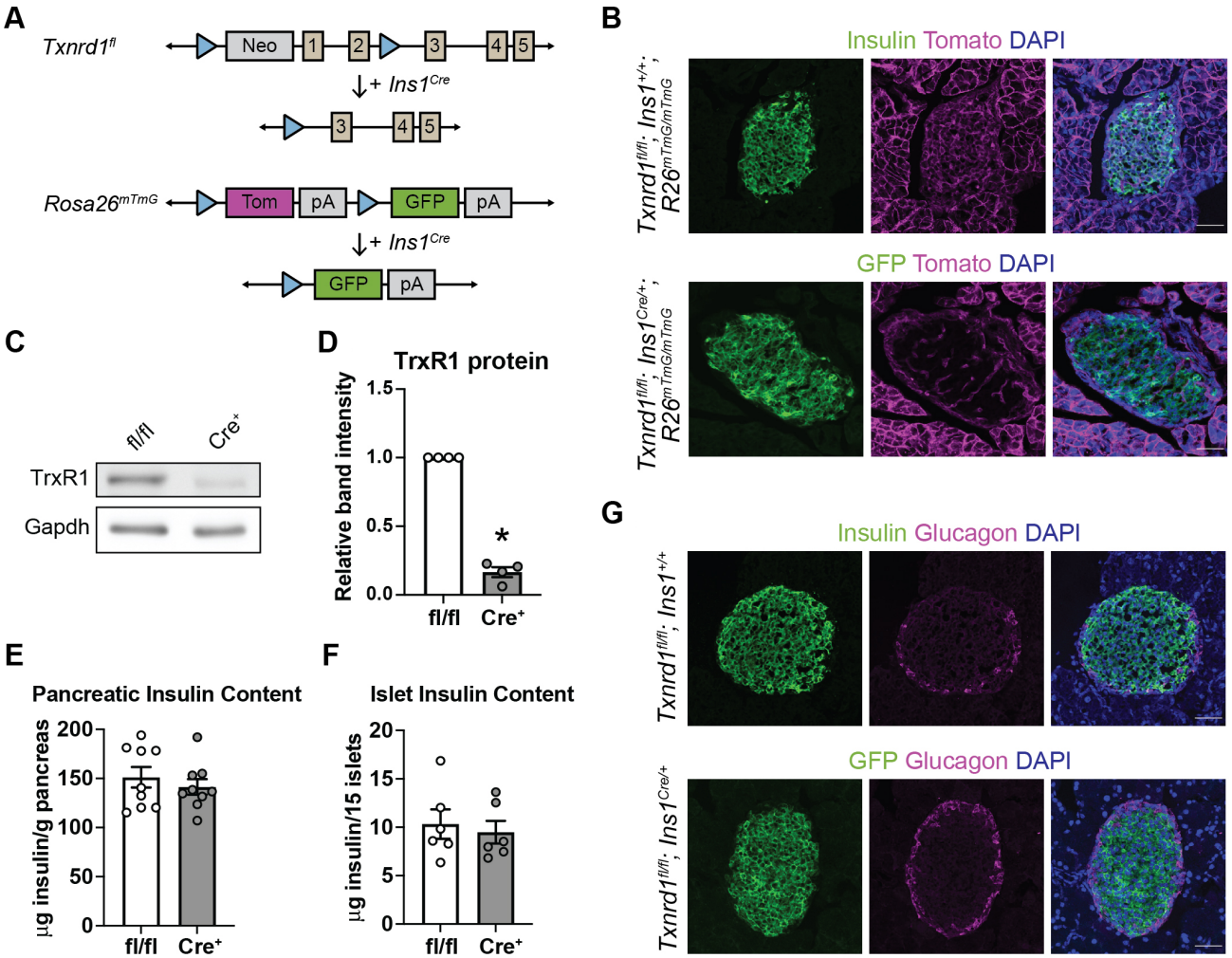

Figure 1. Generation of mice with a β-cell-specific *Txnrd1* knockout. (A) Schematic of alleles used to generate β-cell-specific *Txnrd1* knockout mice that also express a fluorescent Cre-reporter allele. (B) Representative images from pancreatic sections of *Txnrd1*$^{fl/fl}$, *Ins1*$^{+/+}$, *R26*$^{mTmG/mTmG}$ (control) or *Txnrd1*$^{fl/fl}$, *Ins1*$^{Cre/+}$, *R26*$^{mTmG/mTmG}$ (knockout) mice showing native fluorescence of GFP and Tomato and immunofluorescence of insulin. DAPI was used to mark nuclei. Scalebar = 50 μm. (C) TrxR1 protein levels as determined by western blot analysis using islets from *Txnrd1*$^{fl/fl}$, *Ins1*$^{+/+}$ (fl/fl) or *Txnrd1*$^{fl/fl}$, *Ins1*$^{Cre/+}$ (Cre^{+}) mice. Gapdh levels were determined to assess protein loading. A representative blot is shown. (D) Quantification of bands shown in (C). (E–F) Pancreatic (E) or islet (F) insulin content in *Txnrd1*$^{fl/fl}$, *Ins1*$^{+/+}$ (fl/fl) or *Txnrd1*$^{fl/fl}$, *Ins1*$^{Cre/+}$ (Cre^{+}) mice. (G) Representative images from pancreatic sections of *Txnrd1*$^{fl/fl}$, *Ins1*$^{+/+}$, *R26*$^{mTmG/mTmG}$ (control) or *Txnrd1*$^{fl/fl}$, *Ins1*$^{Cre/+}$, *R26*$^{mTmG/mTmG}$ (knockout) mice showing native fluorescence of GFP and immunofluorescence of insulin and glucagon. DAPI was used to mark nuclei. Scalebar = 50 μm. Error bars represent SEM. Results are the average of 3–9 independent experiments with statistical significance indicated. $^{*}P < 0.05$ (vs. fl/fl).

either sex (Figure 2G). Together, these data suggest that *Txnrd1*-deficient β-cells have reduced function despite having normal insulin content, but compensatory changes in peripheral tissues likely allow for normal glucose homeostasis in βKO mice.

Sensitivity of βKO Islets to Continuously Delivered Oxidants

Similar to our previous results using rat islets,[28] acute inhibition of TrxR by AFN increases the sensitivity of control *Txnrd1*$^{fl/fl}$; *Ins1*$^{+/+}$ (*fl/fl*) mouse islets to hydrogen peroxide, delivered continuously by glucose/glucose oxidase, or to peroxynitrite, delivered by combined treatment with a nitric oxide donor (DPTA/NO) and a redox cycler (menadione), as determined by increased phosphorylation of histone H2AX (γH2AX), a marker for activation of the DNA-damage response (Figure 3A and B). However, βKO islets do not demonstrate increased sensitivity to continuous hydrogen peroxide or to peroxynitrite compared to *fl/fl* islets (Figure 3A and B), suggesting that chronic depletion of this essential antioxidant enzyme may trigger compensatory mechanisms to protect β-cells from ROS.

FACS-purification and RNA-sequencing of *Txnrd1*-deficient β-cells

To determine if *Txnrd1*-deficient β-cells utilize adaptive mechanisms to protect against oxidative damage, we performed RNA-sequencing using FACS-purified KO β-cells compared to *Txnrd1*$^{+/+}$; *Ins1*$^{Cre/+}$ β-cells using the *ROSA26*^{mTmG} fluorescent Cre reporter allele. Both *Txnrd1*$^{+/+}$; *Ins1*$^{Cre/+}$ and βKO mice display GFP expression in islet β-cells and Tomato expression in islet non-β-cells (Figure 4A–C). To determine how removal of *Txnrd1* in β-cells affects the transcriptomes of islet non-β-cells, we performed RNA-sequencing using FACS-purified Tomato^{+} cells in addition to GFP^{+} cells. Assessment of islet hormone expression by RNA-sequencing confirms that the GFP^{+} populations are

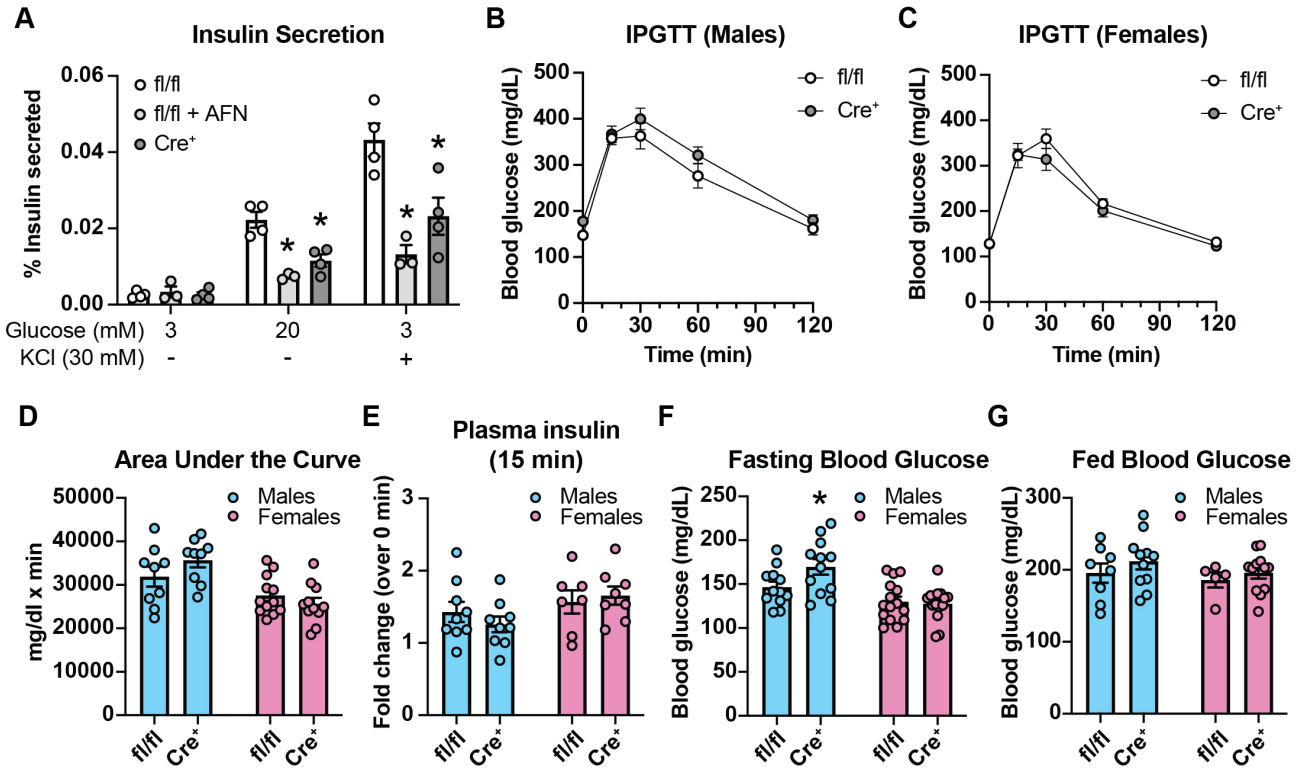

Figure 2. Glucose homeostasis in mice with a β-cell-specific T*xnrd1* knockout. (A) Static insulin secretion following 90-min stimulation with 3 mM glucose, 20 mM glucose, or 30 mM KCl from T*xnrd1*$^{fl/fl}$, *Ins1*$^{+/+}$ (fl/fl) islets with or without 5 μM AFN and from T*xnrd1*$^{fl/fl}$, *Ins1*$^{Cre/+}$ (Cre$^+$) islets. Secretion was normalized to total insulin and is shown as % insulin secreted. (B–C) Intraperitoneal glucose tolerance tests (IPGTT) in male (B) or female (C) T*xnrd1*$^{fl/fl}$, *Ins1*$^{+/+}$ (fl/fl) and T*xnrd1*$^{fl/fl}$, *Ins1*$^{Cre/+}$ (Cre$^+$) mice. (D) Area under the curve measurements for data shown in (B) and (C). (E) Plasma insulin levels in male and female T*xnrd1*$^{fl/fl}$, *Ins1*$^{+/+}$ (fl/fl) and T*xnrd1*$^{fl/fl}$, *Ins1*$^{Cre/+}$ (Cre$^+$) mice before and 15 min following intraperitoneal glucose injection. Results are expressed as fold change over the basal plasma insulin level. (F–G) Blood glucose concentrations following a 4-h fast (F) or following *ad libitum* feeding (G) in male and female T*xnrd1*$^{fl/fl}$, *Ins1*$^{+/+}$ (fl/fl) and T*xnrd1*$^{fl/fl}$, *Ins1*$^{Cre/+}$ (Cre$^+$) mice. Error bars represent SEM. Results are the average of 3–4 independent experiments with statistical significance indicated. *P <0.05 (vs. fl/fl).

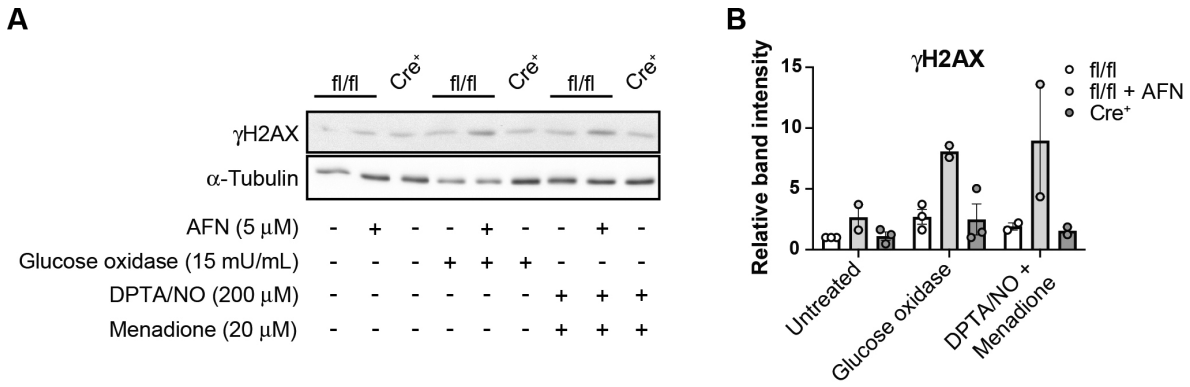

Figure 3: Sensitivity of T*xnrd1*-deficient β-cells to oxidative damage. (A) Phosphorylation of the histone variant H2AX (γH2AX, marker of DNA damage response activation) as assessed by western blot using protein lysates from T*xnrd1*$^{fl/fl}$, *Ins1*$^{+/+}$ (fl/fl) islets with or without 5 μM AFN or from T*xnrd1*$^{fl/fl}$, *Ins1*$^{Cre/+}$ (Cre$^+$) islets following 30 min exposure to hydrogen peroxide delivered continuously by 15 mU/mL glucose oxidase or to 60 min exposure to peroxynitrite, delivered by the combination of DPTA/NO and menadione. α-Tubulin levels were determined to assess protein loading. A representative blot is shown. **(B)** Quantification of bands shown in (A). Error bars represent SEM. Results are the average of 2–3 independent experiments.

enriched for β-cells, and Tomato$^+$ populations are enriched for α-, δ-, and PP-cells, as expected (Figure 4D). Principal component analysis demonstrates that control and T*xnrd1*-deficient GFP$^+$ cells cluster by genotype, suggesting that T*xnrd1*-deficiency alters the β-cell transcriptome (Figure 4E). Indeed, pairwise comparison between control and KO β-cells yielded 266 differentially expressed genes (131 increased and 135 decreased) based on a significance cutoff of |fold change| >2 and adjusted P <0.05 (Figure 4F, Supplementary Table S2). Tomato$^+$ cells from control and βKO mice do not form distinct clusters, suggesting that removal of T*xnrd1* in β-cells does not affect the transcriptomes of islet non-β-cells (Figure 4E). Consistently, only eight genes

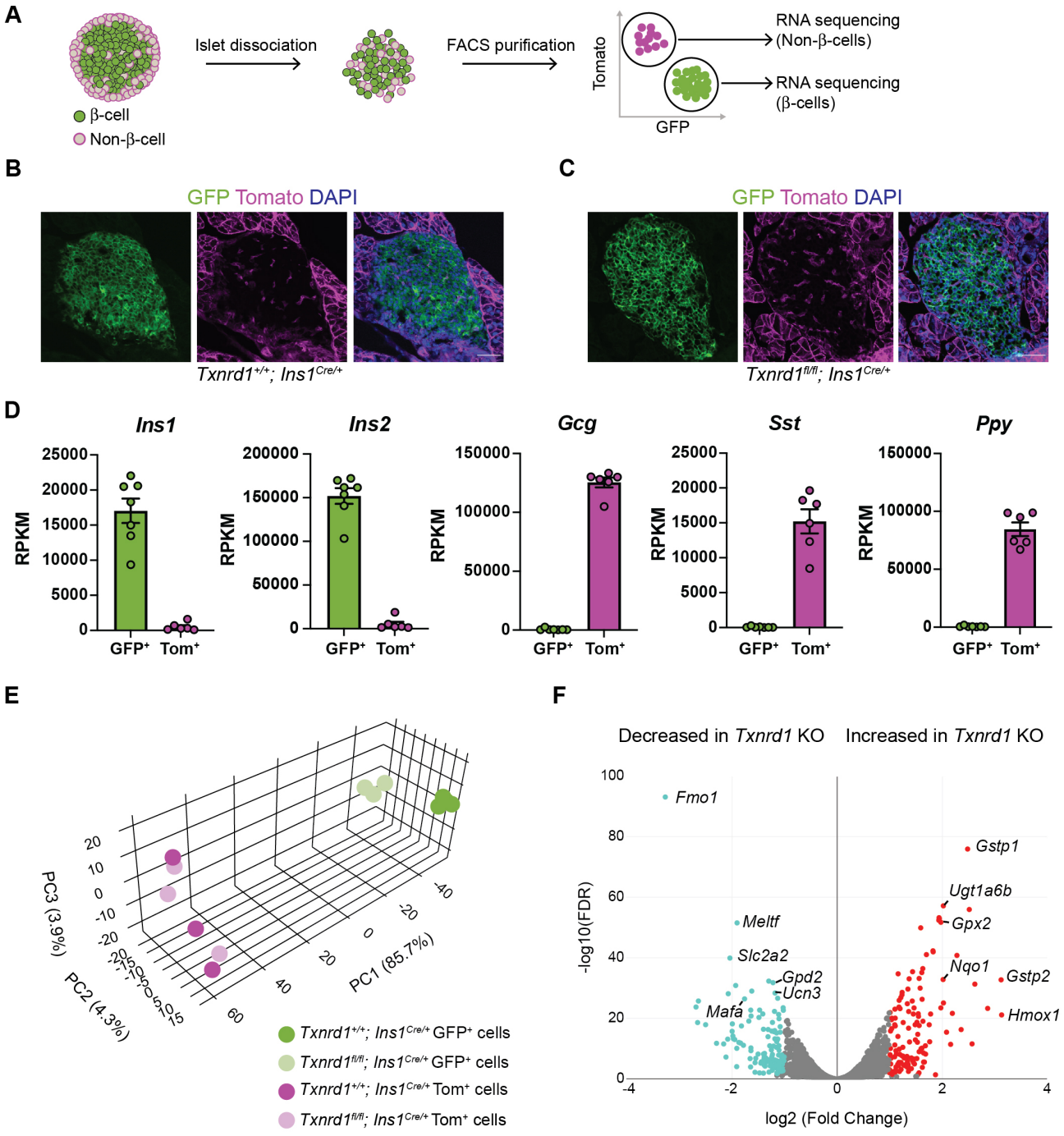

Figure 4. FACS purification and RNA-sequencing of *Txnrd1*-deficient β-cells. (A) Schematic depicting islet dissociation and FACS purification of GFP$^+$ cells and Tomato$^+$ cells from islets expressing the $R26^{mTmG}$ fluorescent Cre reporter allele. (B–C) Representative images from pancreatic sections of $Txnrd1^{+/+}$, $Ins1^{Cre/+}$, $R26^{mTmG/mTmG}$ (B) or $Txnrd1^{fl/fl}$, $Ins1^{Cre/+}$, $R26^{mTmG/mTmG}$ (C) mice showing native fluorescence of GFP and Tomato. DAPI was used to mark nuclei. Scalebar = 50 μm. (D) Expression of *Ins1*, *Ins2*, *Gcg*, Sst, and *Ppy* in the GFP$^+$ and Tomato$^+$ populations as determined by RNA-seq. (E) Principal component analysis of the 13 samples used for RNA-sequencing. (F) Volcano plot showing the number of genes that are significantly changed in *Txnrd1* knockout GFP$^+$ cells compared to control GFP$^+$ cells. Selected genes are named.

(four increased and four decreased) are differentially expressed between Tomato$^+$ cells from control mice compared to Tomato$^+$ cells from βKO mice, and the fold change values are minor compared to the fold change values observed between the two GFP$^+$ populations (Supplementary Figure S1A, Supplementary Table S3). These data demonstrate that chronic β-cell *Txnrd1*-deficiency alters the β-cell transcriptome but does not influence gene expression in islet non-β-cells.

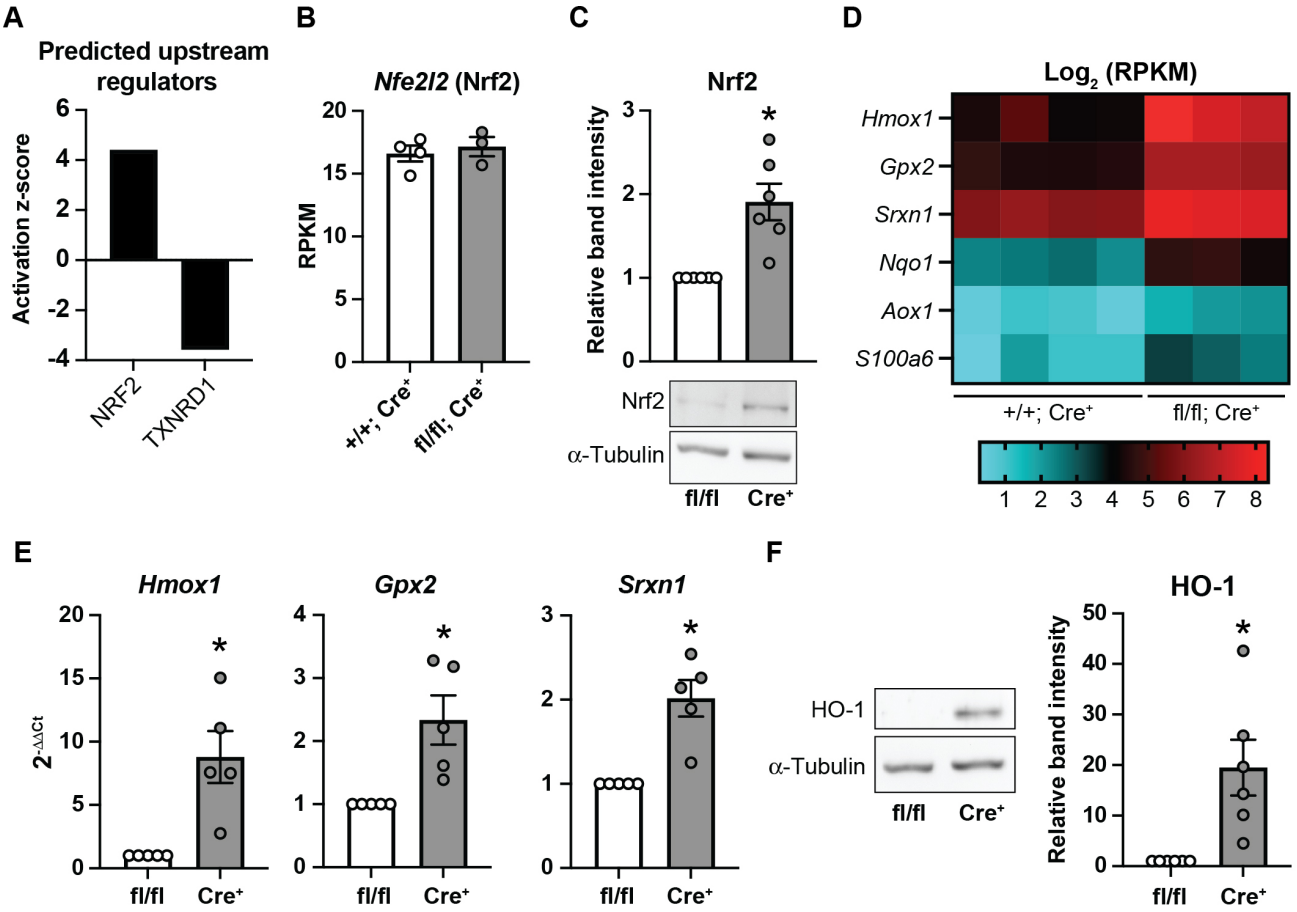

Figure 5. Nrf2 is stabilized in *Txnrd1*-deficient β-cells. (A) Predicted upstream regulators based on significantly changed genes in *Txnrd1* knockout GFP$^+$ cells compared to control GFP$^+$ cells. Analysis was performed using IPA. (B) Expression of *Nfe2l2* in *Txnrd1*$^{+/+}$, *Ins1*$^{Cre/+}$ (+/+; Cre$^+$) or *Txnrd1*$^{fl/fl}$, *Ins1*$^{Cre/+}$ (fl/fl; Cre$^+$) β-cells as determined by RNA-sequencing. (C) Nrf2 protein levels as assessed by western blot in *Txnrd1*$^{fl/fl}$, *Ins1*$^{+/+}$ (fl/fl) and *Txnrd1*$^{fl/fl}$, *Ins1*$^{Cre/+}$ (Cre$^+$) islet lysates. α-Tubulin levels were determined to assess protein loading. Band quantification is shown above a representative blot. (D) Heat map showing Log_2 (RPKM) of selected genes in four *Txnrd1*$^{+/+}$, *Ins1*$^{Cre/+}$ (+/+; Cre$^+$) β-cell samples, and three *Txnrd1*$^{fl/fl}$, *Ins1*$^{Cre/+}$ (fl/fl; Cre$^+$) β-cell samples as determined by RNA-sequencing. All genes shown are significantly different between the genotypes. (E) Expression of *Hmox1*, *Gpx2*, and *Srxn1* in *Txnrd1*$^{fl/fl}$, *Ins1*$^{+/+}$ (fl/fl), and *Txnrd1*$^{fl/fl}$, *Ins1*$^{Cre/+}$ (Cre$^+$) islets as determined by qPCR. (F) HO-1 protein levels as assessed by western blot in *Txnrd1*$^{fl/fl}$, *Ins1*$^{+/+}$ (fl/fl) and *Txnrd1*$^{fl/fl}$, *Ins1*$^{Cre/+}$ (Cre$^+$) islet lysates. α-Tubulin levels were determined to assess protein loading. Band quantification is shown to the right of a representative blot. Results are the average of 3–6 independent experiments with statistical significance indicated. *P $<$0.05 (vs. fl/fl).

Nrf2 is Stabilized in *Txnrd1*-deficient β-cells

Txnrd1 null yeast upregulate genes encoding Prx to compensate for the loss of TrxR.[54] However, *Txnrd1*-deficient β-cells do not increase expression of Prx, Trx, or the mitochondrial TrxR to compensate for the loss of *Txnrd1* (Supplementary Figure S2A and B). To determine which pathways are altered in *Txnrd1*-deficient β-cells that may help them adapt to loss of this essential antioxidant, we utilized Ingenuity Pathway Analysis (IPA) to predict upstream regulators.[55] Based on the genes differentially expressed between KO and control GFP$^+$ cells, IPA predicted activation of nuclear factor erythroid 2 (NFE2)-related factor 2 (Nrf2), a transcription factor that controls expression of many cyto-protective genes,[56] and disruption of Txnrd1 (Figure 5A). Indeed, while *Nfe2l2* (Nrf2) transcript levels were unchanged, βKO islets had significantly increased Nrf2 protein stability compared to controls (Figure 5B and C). This is expected, as Nrf2 is found in a complex with Keap1 and is targeted for degradation. Following Keap1 oxidation, Nrf2 is released allowing for transcriptional regulation. By this mechanism, Nrf2 protein levels are primarily regulated by protein stabilization rather than by increased transcription.[57] Among the most increased genes in KO β-cells are several known Nrf2-targets, including heme oxygenase 1 (*Hmox1*, 9-fold increase), glutathione peroxidase 2 (*Gpx2*, 4-fold increase), sulfiredoxin 1 (*Srxn1*, 3-fold increase), NAD(P)H: quinone oxidoreductase 1 (*Nqo1*, 4-fold increase), aldehyde oxidase (*Aox1*, 2-fold increase), and calcyclin (*S100a6*, 3-fold increase) (Figure 5D).[57–59] Increased mRNA levels of *Hmox1*, *Gpx2*, and *Srxn1* were confirmed by qPCR using βKO islets compared to *fl/fl* controls (Figure 5E). Increased *Hmox* (HO-1) protein levels were confirmed by western blot (Figure 5F). Importantly, non-β-cells from βKO islets have no change in expression of these Nrf2-target genes nor in Prx, Trx, or mitochondrial TrxR (Supplementary Figure S1B), again suggesting that *Txnrd1* knockout in β-cells does not alter gene expression in islet non-β-cells. Together, these data suggest that *Txnrd1*-deficient β-cells have constitutive stability of Nrf2, which may allow them to compensate for the loss of *Txnrd1*. This observation is consistent with previous work demonstrating that *Txnrd1*-deficient hepatocytes display Nrf2 stabilization.[48]

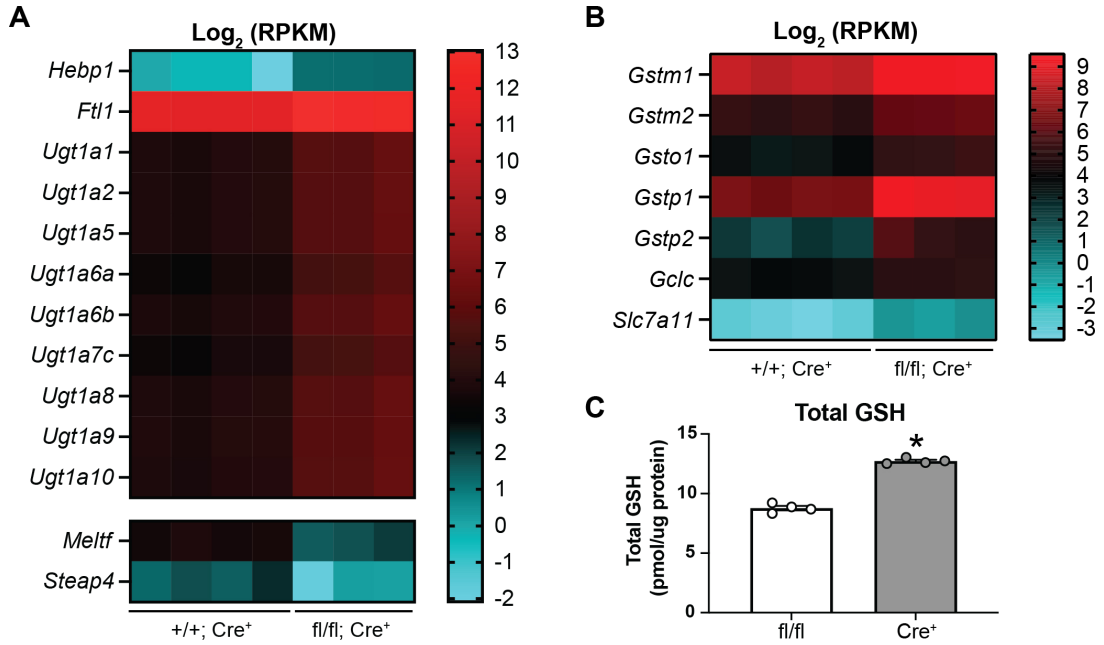

Figure 6. *Txnrd1*-deficient β-cells have altered expression of genes involved in heme metabolism and glutathione metabolism. (A and B) Heat map showing Log_2 (RPKM) of selected genes involved in heme metabolism (A) or glutathione metabolism (B) in $Txnrd1^{+/+}$, $Ins1^{Cre/+}$ (+/+; Cre$^+$) and $Txnrd1^{fl/fl}$, $Ins1^{Cre/+}$ (fl/fl; Cre$^+$) β-cell samples as determined by RNA-sequencing. All genes shown are significantly different between the genotypes. (C) Measurement of total glutathione levels in $Txnrd1^{fl/fl}$, $Ins1^{+/+}$ (fl/fl) and $Txnrd1^{fl/fl}$, $Ins1^{Cre/+}$ (Cre$^+$) islets. Results are the average of 3–4 independent experiments with statistical significance indicated. *P <0.05 (vs. fl/fl).

Txnrd1-deficient β-cells Have Altered Expression of Genes Involved in Heme and Glutathione Metabolism

Txnrd1-deficient β-cells have increased heme oxygenase 1 transcript (*Hmox1*) levels (Figure 5D and E) and protein (HO-1) levels (Figure 5F) compared to controls. Heme oxygenase metabolizes heme to generate biliverdin and bilirubin, both of which have antioxidant properties.[60] However, bilirubin is toxic if not eliminated from the cell, and UDP glucuronosyltransferase (UGT) is the obligatory step of bilirubin elimination.[61] Accordingly, KO β-cells have increased levels (4-fold) of a number of *Ugt1a* transcripts, suggesting that they may have increased levels of bilirubin as a consequence of increased heme metabolism (Figure 6A). Another product of heme metabolism via *Hmox* is free iron.[60] Free iron is pro-oxidant, given its propensity to react with hydrogen peroxide to form the highly reactive hydroxyl radical.[62] *Txnrd1*-deficient β-cells have increased transcript levels of heme binding protein 1 (*Hebp1*, 3-fold increase) and ferritin light polypeptide (*Ftl1*, 3-fold increase), which binds free iron, and decreased transcript levels of melanotransferrin (*Meltf*, 75% decrease) and six-transmembrane epithelial antigen of the prostate family member 4 (*Steap4*, 75% decrease), both of which are involved in iron transport.[63,64] Increased expression of *Hebp1* and *Ftl1* and decreased expression of *Meltf* and *Steap4* suggest compensatory responses to increased heme metabolism in *Txnrd1*-deficient β-cells. Genes involved in glutathione (GSH) biosynthesis and metabolism were also increased in *Txnrd1*-deficient β-cells (Figure 6B). The cysteine/glutamate transporter (*Slc7a11*, 6-fold increase), which mediates the uptake of cysteine, the precursor for GSH biosynthesis, and the catalytic subunit of glutamate-cysteine ligase (*Gclc*, 2-fold increase), the rate-limiting enzyme of GSH biosynthesis, are increased (Figure 6B). The modifier subunit of glutamate-cysteine ligase (*Gclm*) is also increased but did not pass our significance threshold (1.4-fold increase, data not shown). A number of glutathione transferases, including *Gstm1* (2-fold), *Gstm2* (2-fold), *Gsto1* (3-fold), *Gstp1* (6-fold), and *Gstp2* (9-fold), which transfer GSH to target proteins to reduce oxidation, are also increased (Figure 6B). Consistent with the increased expression of genes associated with glutathione synthesis and metabolism, βKO islets have increased total glutathione levels compared to controls (Figure 6C). Together, these observations suggest that *Txnrd1*-deficient β-cells may utilize heme metabolism and glutathione metabolism as protective mechanisms against oxidative damage.

Nrf2 Stabilization Protects β-cells from Oxidants in the Context of *Txnrd1* Disruption

To test the hypothesis that Nrf2-regulated antioxidant mechanisms protect β-cells from oxidative damage in response to TrxR disruption, we utilized a small molecule inhibitor of Nrf2, Aem1.[65] INS 832/13 cells treated with TrxR inhibitor AFN for 3 h have increased stability of Nrf2 and increased expression of HO-1 (Figure 7A and B). Co-treatment with AFN and Aem1 prevents AFN-stimulated stabilization of Nrf2 and increase in expression of HO-1 (Figure 7A and B). Further, co-treatment with AFN and Aem1 sensitizes INS 832/13 cells to hydrogen peroxide delivered continuously by glucose oxidase as compared to treatment with AFN alone (Figure 7C), suggesting that Nrf2-regulated pathways provide protection in β-cells in response to TrxR disruption.

Txnrd1-deficient β-cells Have Decreased Expression of Identity Genes

Among the genes significantly decreased in *Txnrd1*-deficient β-cells are several with roles in maintaining β-cell function and identity, including *Mafa* (70% decrease), a transcription factor controlling β-cell specification and maturation,[66] *Ucn3* (55% decrease), a marker of functionally mature β-cells,[67] *Slc2a2* (75% decrease), encoding the β-cell glucose transporter

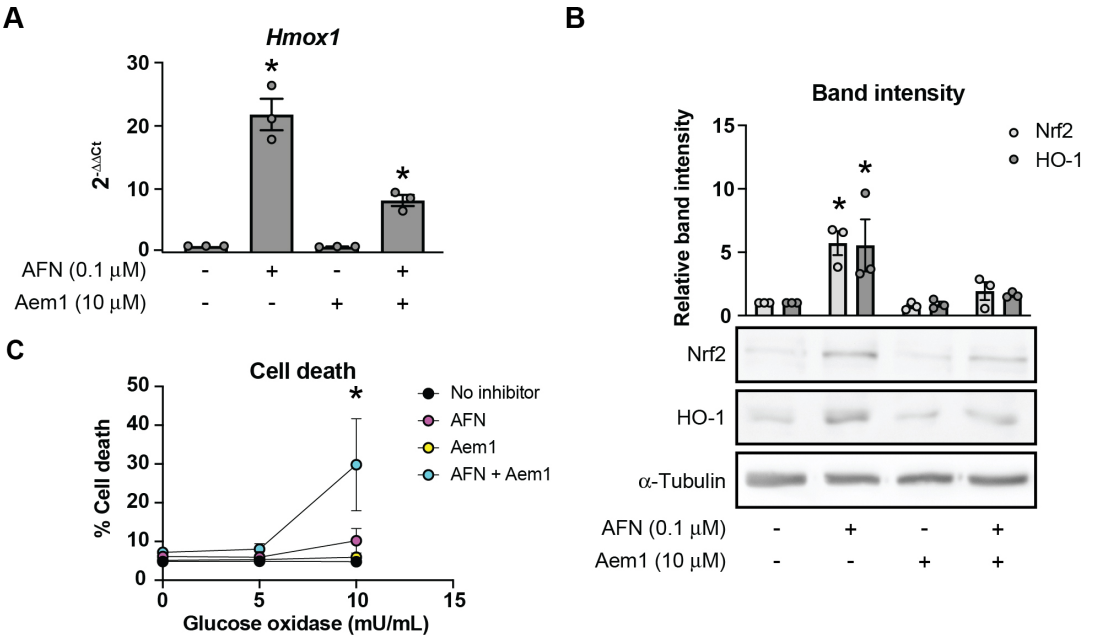

Figure 7. Nrf2 stabilization protects β-cells from oxidants in the context of Txnrd1 disruption. (A and B) *Hmox1* mRNA levels as assessed by qPCR (A), and Nrf2 and HO-1 protein levels as assessed by western blot (B) using lysates from INS 832/13 cells treated for 3 h with TrxR inhibitor AFN, with Nrf2 inhibitor Aem1, or the combination of the two at the indicated concentrations. α-Tubulin levels were determined to assess protein loading in (B). A representative blot is shown below quantification of bands. (C) Death, as determined by Sytox cell death assay, of INS 832/13 cells after 3 h pretreatment with AFN, Aem1, or both together and followed by 4 h treatment with glucose oxidase at the indicated concentrations. Error bars represent SEM. Results are the average of 3–4 independent experiments with statistical significance indicated. *P <0.05 (vs. No inhibitor).

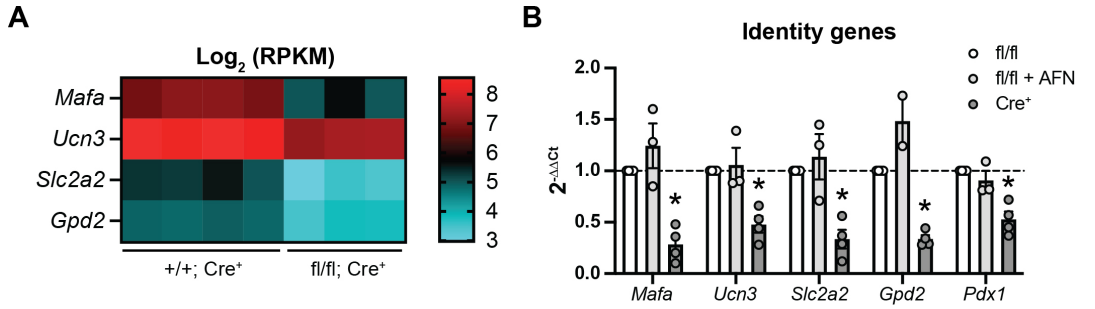

Figure 8. *Txnrd1*-deficient β-cells have reduced expression of identity factors (A) Heat map showing Log_2 (RPKM) of selected β-cell identity genes in $Txnrd1^{+/+}$, $Ins1^{Cre/+}$ (+/+; Cre^+) and $Txnrd1^{fl/fl}$, $Ins1^{Cre/+}$ (fl/fl; Cre^+) β-cell samples as determined by RNA-sequencing. All genes shown are significantly different between the genotypes. (B) Expression of *Mafa*, *Ucn3*, *Slc2a2*, *Gpd2*, and *Pdx1* in $Txnrd1^{fl/fl}$, $Ins1^{+/+}$ (fl/fl) and $Txnrd1^{fl/fl}$, $Ins1^{Cre/+}$ (Cre^+) islets as determined by qPCR. Results are the average of 2–4 independent experiments with statistical significance indicated. *P <0.05 (vs. fl/fl).

Glut2 which helps regulate glucose sensing,[68] and mitochondrial glycerol-3-phosphate dehydrogenase (*Gpd2*, 55% decrease), which, together with the cytosolic *Gpd2*, forms an NADH shuttle system that is necessary for glucose-stimulated insulin secretion[69] (Figure 8A). *Pdx1*, another transcription factor controlling β-cell specification and maintenance of identity,[70] was not significantly decreased in *Txnrd1*-knockout β-cells when assessed by RNA-seq (30% decrease), but was significant when assessed by qPCR using βKO islets compared to *fl/fl* islets, as were the other identity factors (Figure 8B). Decreased mRNA accumulation of these identity genes may explain the mild impairment of insulin secretion observed (Figure 2A). Indeed, functional impairment has previously been observed in models in which *Pdx1*, *Mafa*, or *Slc2a2* are depleted.[66,68,70] Interestingly, however, acute treatment with TrxR inhibitor AFN did not decrease these identity factors (Figure 8B), suggesting that the mechanisms by which acute TrxR inhibition and chronic depletion impair β-cell function are different.

Discussion

In the current study, we generated a mouse model with a pancreatic β-cell-specific knockout of the cytoplasmic isoform of TrxR, *Txnrd1* (Figure 1A–D). This enzyme supports the activity of the Prx/Trx antioxidant cycle by providing reducing equivalents in the form of NADPH to maintain the reduced pool of Trx and Prx. Previous studies from our laboratory have demonstrated that acute inhibition or depletion of *Txnrd1* or of a cytoplasmic isoform of Prx, *Prdx1*, sensitizes a rat insulinoma cell line and rat islets to hydrogen peroxide delivered continuously by glucose/glucose oxidase or to peroxynitrite, but not to hydrogen peroxide delivered as a bolus.[28,31] These previous studies suggest that the cytoplasmic TrxR is necessary for the β-cell defense against continuously-delivered hydrogen peroxide and peroxynitrite and that β-cells may not possess a secondary mechanism to protect themselves should this essential pathway be inhibited. However, islets from mice with a β-cell-

specific knockout of *Txnrd1* (*Txnrd1*$^{fl/fl}$; *Ins1*$^{Cre/+}$, βKO) do not have increased sensitivity to these oxidants, as assessed by the phosphorylation of histone H2AX (γH2AX) (Figure 3). This result suggests that β-cells with a *Txnrd1* knockout may have increased other antioxidant pathways to compensate for the loss of this critical enzyme.

In yeast, loss of TrxR leads to a compensatory increase in genes encoding Prx and Trx.[54] However, increased expression of genes encoding these proteins was not observed in FACS-purified *Txnrd1* knockout β-cells (Supplementary Figure S2). Instead, *Txnrd1* knockout β-cells showed significantly increased expression of Nrf2-regulated cytoprotective genes, an observation that was supported by a significant z-score for NRF2 in an unbiased predicted upstream regulator analysis (Figure 5A and D). Furthermore, while no change in the mRNA levels of Nrf2 (*Nfe2l2*) were observed, βKO islets showed increased levels of Nrf2 protein compared to control islets (Figure 5B and C). Broadly, proteins encoded by Nrf2-regulated genes have roles in protecting the cell from oxidative damage.[56] Among the Nrf2-regulated genes significantly increased in *Txnrd1*-deficient β-cells are *Hmox1*, *Gpx2*, *Srxn1*, and *Nqo1* (Figure 5D). Heme oxygenase metabolizes heme to generate antioxidants biliverdin and bilirubin.[60] *Gpx2* is an antioxidant enzyme that reduces peroxides in the cytoplasm using glutathione as the electron source.[71] In a slow, Trx- and ATP-dependent reaction, *Srxn1* repairs a subset of proteins, in particular Prx, that are over-oxidized by converting the sulfinic acid (via an inferred sulfenic acid intermediate) to a disulfide, which is subsequently rapidly reduced to the dithiol by Trx. This prevents further oxidation to the sulfonic acid, which is an irreversible modification.[72] Quinones are aromatic compounds capable of generating superoxide via "redox cycling."[73] *Nqo1*, or NAD(P)H quinone dehydrogenase 1, reduces quinones to hydroquinones, which is necessary for their detoxification, thus preventing ROS generation.[73]

A deeper look at the genes altered in *Txnrd1*-knockout β-cells suggests a shift from Trx/Prx-based defense mechanisms to mechanisms that rely on biliverdin/bilirubin and/or on glutathione. Indeed, *Txnrd1*-knockout β-cells demonstrate increased expression of transcripts encoding UGT, the enzyme necessary for glucuronidation and elimination of toxic levels of bilirubin (Figure 6A).[61] Furthermore, transcripts encoding proteins involved in glutathione synthesis or proteins that utilize glutathione to reduce oxidized targets are increased in *Txnrd1*-knockout β-cells (Figure 6B), and βKO islets have elevated total glutathione levels compared to controls (Figure 6C). Together, these results suggest that β-cells respond to the loss of TrxR by stabilizing the transcription factor Nrf2, which increases expression of proteins involved in heme- or glutathione-based antioxidant mechanisms. This Nrf2 stabilization in response to *Txnrd1* knockout is not unique to β-cells. Schmidt and colleagues previously observed increased nuclear Nrf2 protein in *Txnrd1*-deficient mouse hepatocytes, as well as increased expression of a similar subset of genes, including *Nqo1*, *Aox1*, *Srxn1*, and a number of glutathione-s-transferases.[48]

The observation that co-treatment with a TrxR inhibitor and a Nrf2 inhibitor renders INS 832/13 cells more sensitive to continuous hydrogen peroxide compared to cells treated with either inhibitor alone suggests that increased Nrf2 stabilization is the reason *Txnrd1*-deficient β-cells appear to have normal survival in response to oxidants (Figure 7C). In support of a protective role for Nrf2 in β-cells, Nrf2 stabilization, by deletion of Nrf2 repressor Keap1, reduces β-cell damage in the context of inducible nitric oxide synthase overexpression,[74] and Nrf2 depletion or knockout increases sensitivity of mouse insulinoma cells or islets to arsenic toxicity.[75] Additional studies, such as combined depletion of *Txnrd1* and *Nrf2*, are necessary to determine the precise role of Nrf2 in the protection observed in βKO islets. Furthermore, since Nrf2 is primarily stabilized under conditions of oxidative stress, but there are no obvious signs of oxidative stress in *Txnrd1*-deficient β-cells, it is unclear how Nrf2 is chronically stabilized. One possibility raised by others is that Nrf2 is directly regulated by TrxR, such that its inhibition or removal stabilizes Nrf2.[48,76,77] Regardless of the mechanism by which Nrf2 is stabilized, our use of a constitutive Cre allele allowed us to observe that *Txnrd1*-knockout β-cells respond to the loss of TrxR by increasing a host of additional cytoprotective genes, suggesting that antioxidant defense is essential for β-cell survival and that the Trx/Prx antioxidant pathway is the primary antioxidant defense mechanism used by β-cells. Use of an inducible Cre recombinase system to recombine the conditional *Txnrd1* allele in adult animals will be important in future studies to avoid developmental adaptive mechanisms and to further test the hypothesis that *Txnrd1* is necessary for the β-cell defense against oxidants *in vivo*.

In addition to its role in the cellular defense against peroxides and peroxynitrite, Trx plays a role in DNA replication by providing electrons to ribonucleotide reductase, the enzyme that converts ribonucleotides to deoxyribonucleotides for DNA synthesis.[52] TrxR plays a role in this process by providing reducing equivalents to Trx in the form of NADPH. Indeed, whole-body knockouts of TrxR die *in utero*.[36] Therefore, we hypothesized that mice with a β-cell-specific knockout of *Txnrd1* may have reduced β-cell mass caused by deletion of TrxR during development. However, no differences in either pancreatic or islet insulin content nor in islet architecture were observed between control and βKO mice, suggesting that *Txnrd1*-deficient β-cells developed a Trx-independent method for DNA replication (Figure 1E–G). This result is consistent with studies in *Txnrd1*-deficient hepatocytes, demonstrating that mammalian cell proliferation can be sustained by either Trx- or glutathione-dependent redox pathways.[78,79] Our observation here of increased expression of genes involved in glutathione synthesis and increased levels of total glutathione in response to TrxR knockout (Figure 6B and C) support the conclusion that *Txnrd1*-deficient β-cells likely adapted during development to rely on glutathione-based redox systems for proliferation. It is also possible that chronic stabilization of Nrf2 promotes β-cell proliferation, allowing for normal insulin content in βKO mice. Indeed, Nrf2 expression is increased in islets in response to high fat diet, a condition that stimulates β-cell mass expansion.[80] Mouse islets depleted of Nrf2 have blunted replication in response to high glucose *ex vivo*, and β-cell mass expansion in response to high fat diet is impaired when Nrf2 is deleted.[80] Further, Nrf2-regulated S100a6, which is significantly increased in *Txnrd1*-deficient β-cells, plays a role in stem cell renewal.[81] Additional studies are necessary to determine the mechanism utilized by *Txnrd1*-knockout β-cells to establish and maintain mass.

Previous work and the current study demonstrate that inhibition of TrxR by AFN significantly blunts glucose- or depolarization-stimulated insulin secretion (Figure 2A).[82] Despite knockout mice maintaining normal whole-body glucose homeostasis (Figure 2B–G), βKO islets have impaired insulin secretion *ex vivo* in response to either high glucose or membrane depolarization (Figure 2A), suggesting that TrxR is necessary for normal β-cell function. However, the mechanism

by which this occurs is unknown. We observed decreased expression of genes encoding proteins involved in maintaining β-cell identity and glucose sensing, including *Mafa*, *Pdx1*, *Ucn3*, *Slc2a2*, and *Gpd2*, in *Txnrd1*-knockout β-cells (Figure 8), which may account for the slight functional impairment. Interestingly, expression and/or function of *Mafa* and *Pdx1* have been shown to be decreased by hydrogen peroxide exposure,[83,84] suggesting that β-cell identity maintenance may be sensitive to changes in redox balance.

While β-cells chronically deficient in *Txnrd1* may be functionally immature, the observation that AFN treatment does not decrease β-cell identity genes (Figure 8B) supports the hypothesis that different mechanisms are responsible for impaired β-cell function in acute vs. chronic TrxR deficiency. Low levels of hydrogen peroxide are thought to promote glucose-stimulated insulin secretion.[85,86] Prx can mediate hydrogen peroxide signaling by transferring oxidizing equivalents from hydrogen peroxide to target proteins through disulfide exchange, a process called a "redox relay."[87] Therefore, it is possible that TrxR mediates this disulfide exchange between Prx and redox-regulated proteins involved in insulin secretion. The observation that depolarization-induced secretion is impaired by AFN suggests that TrxR affects a process downstream of closure of the ATP-sensitive potassium channel. Future studies will be directed at determining which step in the process of glucose-stimulated insulin secretion is impaired by TrxR inhibition.

Together, previous studies and the work presented here suggest that TrxR plays at least two critical roles in pancreatic β-cells.[88] First, TrxR1 is necessary for β-cell protection against ROS, as evidenced by increased sensitivity to oxidative damage when *Txnrd1* is inactivated[28,31] and by upregulation of a number of cytoprotective genes to maintain survival when *Txnrd1* is depleted (current study). Second, TrxR1 is necessary for normal β-cell function and maturation, as evidenced by impaired glucose-stimulated insulin secretion when *Txnrd1* is inhibited or knocked out and by decreased expression of β-cell maturation markers when *Txnrd1* is chronically depleted (current study). This role for TrxR1 in β-cell function provides a compelling explanation for low expression of *Gpx* and catalase in β-cells compared to other tissues,[19–22] given that activity of these antioxidants may interfere with the ability of TrxR1 to promote glucose-stimulated insulin secretion.

Supplementary Material

Supplementary material is available at the *APS Function* online.

Data Availability Statement

Sequencing data from this publication have been deposited in NCBI GEO database under accession number GSE200965.

Acknowledgments

This research was completed in part with technical assistance for RNA-sequencing and analysis from the Genomic Sciences and Precision Medicine Center at MCW, for fluorescence-activated cell sorting from the Flow Cytometry Core at the Versiti Blood Research Institute (Milwaukee, WI, USA), and for tissue imbedding and sectioning from the Children's Research Institute Histology Core at MCW. The authors additionally thank Dr Justin Prigge (Department of Microbiology and Immunology, Montana State University, Bozeman, MT, USA) for technical assistance, and Aaron Naatz, Chay Teng Yeo, and Alyssa Gehant (Department of Biochemistry, Medical College of Wisconsin, Milwaukee, WI, USA) and Dr Neil Hogg (Department of Biophysics, Medical College of Wisconsin, Milwaukee, WI, USA) for helpful discussions related to this project.

Author Contributions

J.S.S. and J.A.C. were responsible for the conception and design of the research. E.E.S. provided animals and materials for this study. J.S.S. and P.A.H. performed the experiments. A.J.M. designed and supervised the RNA-sequencing preparation and analysis. J.S.S., P.A.H., and J.A.C. analyzed the data and interpreted the results of the experiments. J.S.S. prepared the figures and drafted the manuscript. All authors edited and approved the final version of the manuscript and figures. J.S.S. and J.A.C. are the guarantors of this work and, as such, had full access to all the data in the study and take responsibility for the integrity of the data and the accuracy of the data analysis.

Funding

This work was supported by the National Institute of Diabetes and Digestive and Kidney Diseases [grant number K99DK129709 to J.S.S.] and [grant number R01DK052194 to J.A.C.], by the National Institute of Allergy and Infectious Diseases [grant number R01AI044458 to J.A.C.], by a grant from the Medical College of Wisconsin Cancer Center (to J.A.C.), and by a gift from the Forest County Potawatomi Foundation (to J.A.C.). E.E.S. was supported by grants from the National Institute of Diabetes, Digestive and Kidney Diseases [grant number R56/R01DK123738], the National Cancer Institute [grant number R01CA215784], the National Institutes of Health Office of the Director [grant number R21OD026444]; and the National Institutes on Aging [grant number R21AG055022, R01AG040020]. J.S.S. was also supported by the National Heart, Lung, and Blood Institute [grant number T32HL134643].

Conflicts of Interests

No conflicts of interest, financial or otherwise, are declared by the authors.

References

1. Lenzen S. Chemistry and biology of reactive species with special reference to the antioxidative defence status in pancreatic beta-cells. *Biochim Biophys Acta Gen Subj*. 2017;**1861** (8):1929–1942.
2. Nourooz-Zadeh J, Tajaddini-Sarmadi J, McCarthy S, Betteridge DJ, Wolff SP. Elevated levels of authentic plasma hydroperoxides in NIDDM. *Diabetes* 1995;**44** (9):1054–1058.
3. Ghiselli A, Laurenti O, De Mattia G, Maiani G, Ferro-Luzzi A. Salicylate hydroxylation as an early marker of in vivo oxidative stress in diabetic patients. *Free Radical Biol Med* 1992;**13** (6):621–626.
4. Gopaul NK, Anggard EE, Mallet AI, Betteridge DJ, Wolff SP, Nourooz-Zadeh J. Plasma 8-epi-PGF2 alpha levels are elevated in individuals with non-insulin dependent diabetes mellitus. *FEBS Lett* 1995;**368** (2):225–229.
5. Rehman A, Nourooz-Zadeh J, Moller W, Tritschler H, Pereira P, Halliwell B. Increased oxidative damage to all DNA bases

in patients with type II diabetes mellitus. *FEBS Lett* 1999;**448** (1):120–122.
6. Shin CS, Moon BS, Park KS, et al. Serum 8-hydroxy-guanine levels are increased in diabetic patients. *Diabetes Care* 2001;**24** (4):733–737.
7. Sakuraba H, Mizukami H, Yagihashi N, Wada R, Hanyu C, Yagihashi S. Reduced beta-cell mass and expression of oxidative stress-related DNA damage in the islet of Japanese type II diabetic patients. *Diabetologia* 2002;**45** (1):85–96.
8. Ihara Y, Toyokuni S, Uchida K, et al. Hyperglycemia causes oxidative stress in pancreatic beta-cells of GK rats, a model of type 2 diabetes. *Diabetes* 1999;**48** (4):927–932.
9. Tanaka Y, Gleason CE, Tran PO, Harmon JS, Robertson RP. Prevention of glucose toxicity in HIT-T15 cells and Zucker diabetic fatty rats by antioxidants. *Proc Natl Acad Sci U S A* 1999;**96** (19):10857–10862.
10. Dominguez C, Ruiz E, Gussinye M, Carrascosa A. Oxidative stress at onset and in early stages of type 1 diabetes in children and adolescents. *Diabetes Care* 1998;**21** (10):1736–1742.
11. Kalyanaraman B, Hardy M, Podsiadly R, Cheng G, Zielonka J. Recent developments in detection of superoxide radical anion and hydrogen peroxide: opportunities, challenges, and implications in redox signaling. *Arch Biochem Biophys* 2017;**617**:38–47. doi:10.1016/j.abb.2016.08.021.
12. Munro D, Treberg JR. A radical shift in perspective: mitochondria as regulators of reactive oxygen species. *J Exp Biol* 2017;**220** (Pt 7):1170–1180.
13. Schuit F, De Vos A, Farfari S, et al. Metabolic fate of glucose in purified islet cells. Glucose-regulated anaplerosis in beta cells. *J Biol Chem* 1997;**272** (30):18572–18579.
14. Jitrapakdee S, Wutthisathapornchai A, Wallace JC, MacDonald MJ. Regulation of insulin secretion: role of mitochondrial signalling. *Diabetologia* 2010;**53** (6):1019–1032.
15. MacDonald MJ, Fahien LA, Brown LJ, Hasan NM, Buss JD, Kendrick MA. Perspective: emerging evidence for signaling roles of mitochondrial anaplerotic products in insulin secretion. *Am J Physiol Endocrinol Metab* 2005;**288** (1):E1–E15.
16. Matschinsky FM. Banting Lecture 1995. A lesson in metabolic regulation inspired by the glucokinase glucose sensor paradigm. *Diabetes* 1996;**45** (2):223–241.
17. Robertson RP, Harmon J, Tran PO, Poitout V. Beta-cell glucose toxicity, lipotoxicity, and chronic oxidative stress in type 2 diabetes. *Diabetes* 2004;**53** (suppl_1):S119–S124.
18. Maritim AC, Sanders RA, Watkins JB 3rd. Diabetes, oxidative stress, and antioxidants: a review. *J Biochem Mol Toxicol* 2003;**17** (1):24–38.
19. Grankvist K, Marklund SL, Taljedal IB. CuZn-superoxide dismutase, Mn-superoxide dismutase, catalase and glutathione peroxidase in pancreatic islets and other tissues in the mouse. *Biochem J* 1981;**199** (2):393–398.
20. Tiedge M, Lortz S, Munday R, Lenzen S. Complementary action of antioxidant enzymes in the protection of bioengineered insulin-producing RINm5F cells against the toxicity of reactive oxygen species. *Diabetes* 1998;**47** (10):1578–1585.
21. Lenzen S, Drinkgern J, Tiedge M. Low antioxidant enzyme gene expression in pancreatic islets compared with various other mouse tissues. *Free Radical Biol Med* 1996;**20** (3):463–466.
22. Lenzen S. Oxidative stress: the vulnerable beta-cell. *Biochem Soc Trans* 2008;**36** (Pt 3):343–347.
23. Kubisch HM,Wang J,Luche R, et al. Transgenic copper/zinc superoxide dismutase modulates susceptibility to type I diabetes. *Proc Natl Acad Sci U S A* 1994;**91** (21):9956–9959.
24. Benhamou PY, Moriscot C, Richard MJ, et al. Adenovirus-mediated catalase gene transfer reduces oxidant stress in human, porcine and rat pancreatic islets. *Diabetologia* 1998;**41** (9):1093–1100.
25. Xu B, Moritz JT, Epstein PN. Overexpression of catalase provides partial protection to transgenic mouse beta cells. *Free Radical Biol Med* 1999;**27** (7-8):830–837.
26. Harmon JS, Bogdani M, Parazzoli SD, et al. beta-Cell-specific overexpression of glutathione peroxidase preserves intranuclear MafA and reverses diabetes in db/db mice. *Endocrinology* 2009;**150** (11):4855–4862.
27. Hotta M,Tashiro F,Ikegami H, et al. Pancreatic beta cell-specific expression of thioredoxin, an antioxidative and antiapoptotic protein, prevents autoimmune and streptozotocin-induced diabetes. *J Exp Med* 1998;**188** (8):1445–1451.
28. Stancill JS, Broniowska KA, Oleson BJ, Naatz A, Corbett JA. Pancreatic beta-cells detoxify H2O2 through the peroxiredoxin/thioredoxin antioxidant system. *J Biol Chem* 2019;**294** (13):4843–4853.
29. Stancill JS, Osipovich AB, Cartailler JP, Magnuson MA. Transgene-associated human growth hormone expression in pancreatic beta-cells impairs identification of sex-based gene expression differences. *Am J Physiol Endocrinol Metab* 2019;**316** (2):E196–E209.
30. Rhee SG, Chae HZ, Kim K. Peroxiredoxins: a historical overview and speculative preview of novel mechanisms and emerging concepts in cell signaling. *Free Radical Biol Med* 2005;**38** (12):1543–1552.
31. Stancill JS, Happ JT, Broniowska KA, Hogg N, Corbett JA. Peroxiredoxin 1 plays a primary role in protecting pancreatic beta-cells from hydrogen peroxide and peroxynitrite. *Am J Physiol Regul Integr Comp Physiol* 2020;**318** (5):R1004–R1013.
32. Minn AH, Hafele C, Shalev A. Thioredoxin-interacting protein is stimulated by glucose through a carbohydrate response element and induces beta-cell apoptosis. *Endocrinology* 2005;**146** (5):2397–2405.
33. Chen J, Hui ST, Couto FM, et al. Thioredoxin-interacting protein deficiency induces Akt/Bcl-xL signaling and pancreatic beta-cell mass and protects against diabetes. *FASEB J* 2008;**22** (10):3581–3594.
34. Chen J, Saxena G, Mungrue IN, Lusis AJ, Shalev A. Thioredoxin-interacting protein: a critical link between glucose toxicity and beta-cell apoptosis. *Diabetes* 2008;**57** (4):938–944.
35. Minireview Shalev A. Thioredoxin-interacting protein: regulation and function in the pancreatic beta-cell. *Mol Endocrinol* 2014;**28** (8):1211–1220.
36. Bondareva AA, Capecchi MR, Iverson SV, et al. Effects of thioredoxin reductase-1 deletion on embryogenesis and transcriptome. *Free Radical Biol Med* 2007;**43** (6):911–923.
37. Muzumdar MD, Tasic B, Miyamichi K, Li L, Luo L. A global double-fluorescent Cre reporter mouse. *Genesis* 2007;**45** (9):593–605.
38. Thorens B, Tarussio D, Maestro MA, Rovira M, Heikkila E, Ferrer J. Ins1(Cre) knock-in mice for beta cell-specific gene recombination. *Diabetologia* 2015;**58** (3):558–565.
39. Hohmeier HE, Mulder H, Chen G, Henkel-Rieger R, Prentki M, Newgard CB. Isolation of INS-1-derived cell lines with robust ATP-sensitive K+ channel-dependent and -independent glucose-stimulated insulin secretion. *Diabetes* 2000;**49** (3):424–430.

40. Kelly CB, Blair LA, Corbett JA, Scarim AL. Isolation of islets of Langerhans from rodent pancreas. *Methods Mol Med* **83**;2003:(3–14). doi: 10.1385/1-59259-377-1:003.
41. Broniowska KA, Oleson BJ, McGraw J, Naatz A, Mathews CE, Corbett JA. How the location of superoxide generation influences the beta-cell response to nitric oxide. *J Biol Chem* 2015;**290** (12):7952–7960.
42. Oleson BJ, Broniowska KA, Naatz A, Hogg N, Tarakanova VL, Corbett JA. Nitric oxide suppresses beta-cell apoptosis by inhibiting the DNA damage response. *Mol Cell Biol* 2016;**36** (15):2067–2077.
43. Montana E, Bonner-Weir S, Weir GC. Beta cell mass and growth after syngeneic islet cell transplantation in normal and streptozocin diabetic C57BL/6 mice. *J Clin Invest* 1993;**91** (3):780–787.
44. Heitmeier MR, Scarim AL, Corbett JA. Interferon-gamma increases the sensitivity of islets of Langerhans for inducible nitric-oxide synthase expression induced by interleukin 1. *J Biol Chem* 1997;**272** (21):13697–13704.
45. Kalari KR, Nair AA, Bhavsar JD, et al. MAP-RSeq: mayo Analysis Pipeline for RNA sequencing. *BMC Bioinf* 2014;**15** (1):224.
46. Robinson MD, McCarthy DJ, Smyth GK. edgeR: a bioconductor package for differential expression analysis of digital gene expression data. *Bioinformatics* 2010;**26** (1): 139–140.
47. Nolan T, Hands RE, Bustin SA. Quantification of mRNA using real-time RT-PCR. *Nat Protoc* 2006;**1** (3):1559–1582.
48. Suvorova ES, Lucas O, Weisend CM, et al. Cytoprotective Nrf2 pathway is induced in chronically txnrd 1-deficient hepatocytes. *PLoS One* 2009;**4** (7):e6158.
49. Khan P, Idrees D, Moxley MA, et al. Luminol-based chemiluminescent signals: clinical and non-clinical application and future uses. *Appl Biochem Biotechnol* 2014;**173** (2):333–355.
50. Tietze F. Enzymic method for quantitative determination of nanogram amounts of total and oxidized glutathione: applications to mammalian blood and other tissues. *Anal Biochem* 1969;**27** (3):502–522.
51. Iverson SV, Eriksson S, Xu J, et al. A Txnrd1-dependent metabolic switch alters hepatic lipogenesis, glycogen storage, and detoxification. *Free Radical Biol Med* 2013;**63**:369–380. doi: 10.1016/j.freeradbiomed.2013.05.028.
52. Laurent TC, Moore EC, Reichard P. Enzymatic synthesis of deoxyribonucleotides. Iv. isolation and characterization of thioredoxin, the hydrogen donor from *Escherichia coli* B. *J Biol Chem* 1964;**239** (10):3436–3444.
53. Matsui M, Oshima M, Oshima H, et al. Early embryonic lethality caused by targeted disruption of the mouse thioredoxin gene. *Dev Biol* 1996;**178** (1):179–185.
54. Carmel-Harel O, Stearman R, Gasch AP, Botstein D, Brown PO, Storz G. Role of thioredoxin reductase in the Yap1p-dependent response to oxidative stress in *Saccharomyces cerevisiae*. *Mol Microbiol* 2001;**39** (3):595–605.
55. Kramer A, Green J, Pollard J, Tugendreich S. Causal analysis approaches in ingenuity pathway analysis. *Bioinformatics* 2014;**30** (4):523–530.
56. Nguyen T, Nioi P, Pickett CB. The Nrf2-antioxidant response element signaling pathway and its activation by oxidative stress. *J Biol Chem* 2009;**284** (20):13291–13295.
57. Tonelli C, Chio IIC, Tuveson DA. Transcriptional regulation by Nrf2. *ARS* 2018;**29** (17):1727–1745.
58. Maeda K, Ohno T, Igarashi S, Yoshimura T, Yamashiro K, Sakai M. Aldehyde oxidase 1 gene is regulated by Nrf2 pathway. *Gene* 2012;**505** (2):374–378.
59. Lesniak W, Szczepanska A, Calcyclin Kuznicki J. Calcyclin (S100A6) expression is stimulated by agents evoking oxidative stress via the antioxidant response element. *Biochim Biophys Acta* 2005;**1744** (1):29–37.
60. Ryter SW, Tyrrell RM. The heme synthesis and degradation pathways: role in oxidant sensitivity. Heme oxygenase has both pro- and antioxidant properties. *Free Radical Biol Med* 2000;**28** (2):289–309.
61. Bosma PJ, Seppen J, Goldhoorn B, et al. Bilirubin UDP-glucuronosyltransferase 1 is the only relevant bilirubin glucuronidating isoform in man. *J Biol Chem* 1994;**269** (27):17960–17964.
62. Aust SD, Morehouse LA, Thomas CE. Role of metals in oxygen radical reactions. *J Free Radic Biol Med* 1985;**1** (1):3–25.
63. Kennard ML, Richardson DR, Gabathuler R, Ponka P, Jefferies WA. A novel iron uptake mechanism mediated by GPI-anchored human p97. *EMBO J* 1995;**14** (17): 4178–4186.
64. Ohgami RS, Campagna DR, McDonald A, Fleming MD. The steap proteins are metalloreductases.*Blood* 2006;**108** (4):1388–1394.
65. Bollong MJ, Yun H, Sherwood L, Woods AK, Lairson LL, Schultz PG. A small molecule inhibits deregulated NRF2 transcriptional activity in cancer. *ACS Chem Biol* 2015;**10** (10):2193–2198.
66. Zhang C, Moriguchi T, Kajihara M, et al. MafA is a key regulator of glucose-stimulated insulin secretion.*Mol Cell Biol* 2005;**25** (12):4969–4976.
67. Blum B, Hrvatin S, Schuetz C, Bonal C, Rezania A, Melton DA. Functional beta-cell maturation is marked by an increased glucose threshold and by expression of urocortin 3. *Nat Biotechnol* 2012;**30** (3):261–264.
68. Guillam MT, Hummler E, Schaerer E, et al. Early diabetes and abnormal postnatal pancreatic islet development in mice lacking Glut-2. *Nat Genet* 1997;**(17)** (3):327–330.
69. Eto K, Tsubamoto Y, Terauchi Y, et al. Role of NADH shuttle system in glucose-induced activation of mitochondrial metabolism and insulin secretion.*Science* 1999;**283** (5404):981–985.
70. Gao T, McKenna B, Li C, et al. Pdx1 maintains beta cell identity and function by repressing an alpha cell program. *Cell Metab* 2014;**19** (2):259–271.
71. Chu FF, Doroshow JH, Esworthy RS. Expression, characterization, and tissue distribution of a new cellular selenium-dependent glutathione peroxidase, GSHPx-GI. *J Biol Chem* 1993;**268** (4):2571–2576.
72. Biteau B, Labarre J, Toledano MB. ATP-dependent reduction of cysteine-sulphinic acid by *S. cerevisiae* sulphiredoxin. *Nature* 2003;**425** (6961):980–984.
73. Ross D, Siegel D. The diverse functionality of NQO1 and its roles in redox control. *Redox Biol* 2021;**41**:101950. doi: 10.1016/j.redox.2021.101950.
74. Yagishita Y, Fukutomi T, Sugawara A, et al. Nrf2 protects pancreatic beta-cells from oxidative and nitrosative stress in diabetic model mice. *Diabetes* 2014;**63** (2): 605–618.
75. Yang B, Fu J, Zheng H, et al. Deficiency in the nuclear factor E2-related factor 2 renders pancreatic beta-cells vulnerable to arsenic-induced cell damage.*Toxicol Appl Pharmacol* 2012;**264** (3):315–323.
76. Cebula M,Schmidt EE,Arner ES. TrxR1 as a potent regulator of the Nrf2-Keap1 response system. *Antioxid Redox Signal* 2015;**23** (10):823–853.

77. Schmidt EE. Interplay between cytosolic disulfide reductase systems and the Nrf2/Keap1 pathway. *Biochem Soc Trans* 2015;**43** (4):632–638.
78. Rollins MF, van der Heide DM, Weisend CM, et al. Hepatocytes lacking thioredoxin reductase 1 have normal replicative potential during development and regeneration. *J Cell Sci* 2010;**123** (Pt 14):2402–2412.
79. Prigge JR, Eriksson S, Iverson SV, et al. Hepatocyte DNA replication in growing liver requires either glutathione or a single allele of txnrd1. *Free Radical Biol Med* 2012;**52** (4): 803–810.
80. Baumel-Alterzon S, Katz LS, Brill G, et al. Nrf2 Regulates beta-cell Mass by suppressing beta-cell death and promoting beta-cell proliferation. *Diabetes* 2022;**71** (5):989–1011.
81. Grahn THM, Niroula A, Vegvari A, et al. S100A6 is a critical regulator of hematopoietic stem cells. *Leukemia* 2020;**34** (12):3323–3337.
82. Cohen-Kutner M, Khomsky L, Trus M, et al. Thioredoxin-mimetic peptides (TXM) reverse auranofin induced apoptosis and restore insulin secretion in insulinoma cells. *Biochem Pharmacol* 2013;**85** (7):977–990.
83. Guo S, Dai C, Guo M, et al. Inactivation of specific beta cell transcription factors in type 2 diabetes. *J Clin Invest* 2013;**123** (8):3305–3316.
84. Leenders F, Groen N, de Graaf N, et al. Oxidative stress leads to beta-cell dysfunction through loss of beta-cell identity. *Front Immunol* 2021;**12**:690379. doi:10.3389/fimmu.2021.690379.
85. Pi J, Bai Y, Zhang Q, et al. Reactive oxygen species as a signal in glucose-stimulated insulin secretion. *Diabetes* 2007;**56** (7):1783–1791.
86. Leloup C, Tourrel-Cuzin C, Magnan C, et al. Mitochondrial reactive oxygen species are obligatory signals for glucose-induced insulin secretion.*Diabetes* 2009;**58** (3): 673–681.
87. Sobotta MC, Liou W, Stocker S, et al. Peroxiredoxin-2 and STAT3 form a redox relay for H2O2 signaling. *Nat Chem Biol* 2015;**11** (1):64–70.
88. Stancill JS,Corbett JA. The Role of thioredoxin/peroxiredoxin in the beta-cell defense against oxidative damage. *Front Endocrinol (Lausanne)* 2021;**12**:718235. doi: 10.3389/fendo.2021.718235.